American Journal of Environmental Engineering 2022, 12(1): 1-8
DOI: 10.5923/j.ajee.20221201.01

Estimation of Drag Coefficient in a Meandering Gravel-Bed River with Vegetated Banks

Sina Sohrabi[1], Hossein Afzalimehr[1,*], Vijay P. Singh[2]

[1]Dept. of Civil Engineering, Iran Univ. of Science and Technology, Narmak, Tehran, Iran
[2]Regents Professor and Caroline & William N. Lehrer Distinguished Chair in Water Engineering, Dept. of Biological and Agricultural Engineering and Zachry Dept. of Civil & Enviv. Engineering, Texas. A&M Univ., College Station, TX, USA

Abstract This paper investigates the effect of hydraulic parameters in the flow resistance estimation in a meander river with gravel bed and vegetated banks. Data collection was carried out in a meandering reach in the river Deryouk located in northern Iran. The selected reach was 28 m long and with large aspect ratio (large width /small flow depth). In addition, eight cross sections of this reach were selected to measure 29 velocity profiles and the main geometric parameters. Results showed that for a large aspect ratio, the maximum velocity occurs under the water surface near the vegetated bank. Disorder velocity profiles were observed more in the regions with dense vegetation canopies. The parabolic method can be used to estimate shear velocity near the vegetated banks for all cross sections. Drag coefficient changes considerably with the vegetation density along the selected meandering reach. The Reynolds number shows an inverse relation with drag coefficient.

Keywords Flow resistance, Drag coefficient, Vegetated bank, Parabolic method, Shear velocity

1. Introduction

River restoration and fluvial processes determine riparian zone of rivers. Rivers stability and effects of climate change on rivers are the most remarkable issues about river management. However, the changes which made by human on the morphodynamics of the rivers usually may play opposite effect on River restoration and management. For example, removing the vegetation of river bank is one of the common solution for decreasing the probability of flood risk. However, the vegetation can reduce the flow velocity, decreasing the transport sedimentation and erosion within the vegetated patch (Green, 2006; Luhar et al., 2008; Nepf and Ghisalberti, 2008; Nikora et al., 2008; Zong and Nepf, 2010; Meire et al., 2014). The vegetated banks have much stability than the bare banks (Afzalimehr and Dey, 2009; Pollen and Simon, 2005). Rivers, especially in mountain regions develop a winding course rather than straight path (Camporeale et al., 2005; Mohanty et al., 2022). Therefore, investigate the flow resistance in meandering rivers is important.

Vegetation canopy deflect the flow towards the bare bed and banks increasing the average flow velocity at these regions. The average velocity decreased around and within the vegetation canopy and the lateral gradients velocity occurs in banks of sections with vegetation and without canopy, generating the extreme shear layer at the banks (Johannesson and Parker, 1989). On the other hand, secondary flow occurred in meandering rivers affect the velocity and shear velocity values which calculate the resistance to flow. Also, the velocity distribution changes near the vegetated banks generating the dip phenomenon near the vegetated bank (Afzalimehr and Dey, 2009). Many researchers, (e.g., Liu and et al., 2016; Li and et al., 2021), reported that the vegetation affects the secondary flows, turbulence intensities and Reynolds shear stresses in meandering rivers. Interaction of the primary and the secondary flows on the velocity distribution in meandering rivers, provide probability of growing the submerged and emergent canopies and deposition along the river banks.

Flow resistance is the one of the most key topics in the river engineering to use in the hydraulic and hydrodynamics calculations related to the hydraulic structures design, bed forms changes, flooding management, deposition and sediment transport patterns. Generally, the flow resistance of rivers depends on the bed and banks conditions. Therefore, vegetated banks impact on the flow resistance, drag force and erosion around them (Järvelä, 2002; James et al., 2008; Tahershamsi et al., 2018). Also, the presence of the canopies along the floodplain causes extra flow resistance changing deposition and sediment transport rate in the meandering rivers (Ismail and Shiono, 2006).

The objective of this study is to estimate drag coefficient along a meandering reach with gravel bed and vegetated banks by applying the parabolic law.

* Corresponding author:
hafzali@iust.ac.ir (Hossein Afzalimehr)
Received: Apr. 17, 2022; Accepted: May 6, 2022; Published: May 24, 2022
Published online at http://journal.sapub.org/ajee

2. Materials and Methods

The experimental data were measured in Deryouk river in the northern Iran. This gravel bed meandering river is located 40 kilometers away from the Amol city in the north of Iran. A reach with 28m length where started at end of bending section selected for estimating the flow resistance in this reach of river with vegetated banks. In addition, eight cross sections for the selected reach was used to measure the vertical velocity distribution (Fig. 1). The vegetated banks are prevalent along the both side of the reach with different densities. However, density of canopies get lower at the outer bank of the meander. Because of the impact of vegetation on the point velocities, the selected cross sections for measuring the velocity vertical distribution placed at 0.2, 1.55, 3.8, 7.71, 10.63, 17.28, 23.95 and 24.5 m away from beginning of the reach (Fig. 2). The aspects ratio (width/flow depth ratio) of the selected cross sections was in the range between 23 and 30.

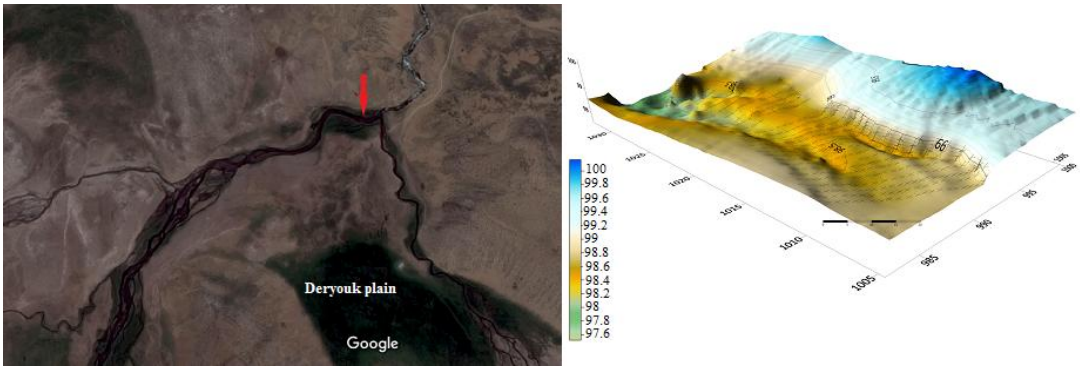

Figure 1. Location of Deryouk river and plan of the selected reach

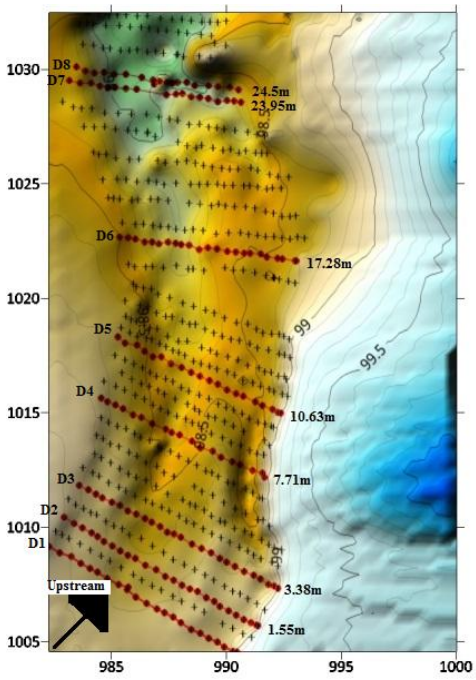

Figure 2. Cross sections to measure data

The median diameter of sediment particles was d_{50} = 33 mm calculated by using Wolman method (1954) and the standard deviation of selected reach was σ_g = 1.44. showing the bed material are uniform. The grain size distribution of the bed material of the selected reach was presented in figure 3.

Four velocity profiles were measured at each cross section. Most of them were near the vegetated banks in order to estimate the shear velocity and resistance to flow. Accordingly, 29 velocity profiles were measured to estimate flow resistance. The vertical distance between velocity profiles depends on the location of the measuring velocity from the vegetated banks. Because of the current-meter diameter is 5 cm, the minimum distance from the bed to measure the point velocity will be 2.5 cm. Figure 4 shows the velocity measurement with butterfly current meter and the cross sections with vegetated banks.

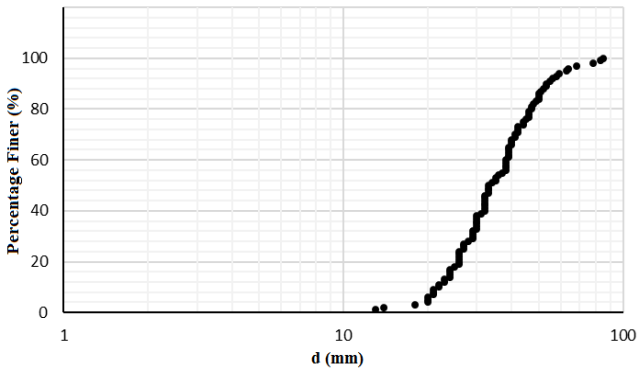

Figure 3. Grain size of distribution

Figure 4. Velocity measurement in the reach with vegetated banks

2.1. Estimate Flow Resistance

In this study, the flow resistance in the present of vegetated banks were estimated by the equation (1) as follows:

$$\frac{U}{u^*} = \frac{R^{4/3}}{ng^{1/2}} = \left(\frac{2}{C_D}\right)^{1/2} \quad (1)$$

Where, U is the mean velocity of cross section, u^* is the shear velocity, R is the hydraulic radius, g is the gravity acceleration, n is the Manning coefficient and C_D is the drag coefficient. The mean velocity of each cross section was calculated by the velocity measurements at each cross section axis (u_p) and then the cross sectional mean velocity (U) was calculated as follows:

$$U = \frac{\sum_{i=1}^{n} A_i u_i}{A} \quad (2)$$

2.2. Shear Velocity Methods

The shear velocity of each cross section was calculated by two methods in this study, the boundary layer characteristics method and the parabolic law.

2.2.1. Boundary Layer Characteristics Method

In this method (Azalimehr and Anctil, 2000), all the point velocities in each profile are used to calculate shear velocity (u^*) as follows:

$$u^* = \frac{U_{max}(\delta^* - \theta)}{4.4\delta^*} \quad (3)$$

In which U_{max} in the maximum velocity in each profile, the displacement thickness of boundary layer (δ^*) and the momentum thickness of boundary layer (Θ) are calculated by equation (4) and (5), respectively.

$$\delta^* = \int_0^h \left(1 - \frac{u}{U_{max}}\right) dh \quad (4)$$

$$\Theta = \int_0^h \frac{u}{U_{max}} \left(1 - \frac{u}{U_{max}}\right) dh \quad (5)$$

Where, h is the depth of chosen axis, u is point velocity and U_{max} is the maximum velocity of velocity profile.

2.2.2. Parabolic Method

Each velocity profile can be divided in two regions, the inner and the outer. The near region composes of 20% of the bed near the bed and the outer region is formed by 80% near the water surface. Afzalimehr and Anctil 1999 and 2000 showed that the inner region data can be presented by the logarithmic law and the outer one by the parabolic law. The logarithmic law gets deviated after the edge of the inner and outer region of the boundary layer of the velocity profile, especially in the presence of the vegetation canopies. Since this study investigates the effect of the bank vegetation on the flow resistance and the near bed region in gravel-bed rivers is not easy to measure by the current-meter, the shear velocity can be calculated the velocity data in the outer region of the boundary layer as follows:

$$\frac{u}{U_{max}} = \Omega\left(1 - \frac{z + ad_{50}}{h + ad_{50}}\right)^2 + \omega \quad (6)$$

Accordingly, the shear velocity was computed from the regression of the $\left(\frac{u}{U_{max}}\right)$ and $\left(1 - \frac{z+ad_{50}}{h+ad_{50}}\right)^2$ of the equation (6). Where Ω is a coefficient equals to the slope of this regression., z is the point distance from the bed, d_{50} is the median diameter of sediment particles, h is the depth of velocity profile, a is modification coefficient of the parabolic law equal 0.2 in this study and the ω is the constant coefficient which equals to intercept of the regression formed between $\left(\frac{u}{U_{max}}\right)$ and $\left(1 - \frac{z+ad_{50}}{h+ad_{50}}\right)^2$.

It is assumed that the variation of bed along the reach is negligible and the flow is steady. Along no change occurs in the vegetation size and the flow condition during the measuring period.

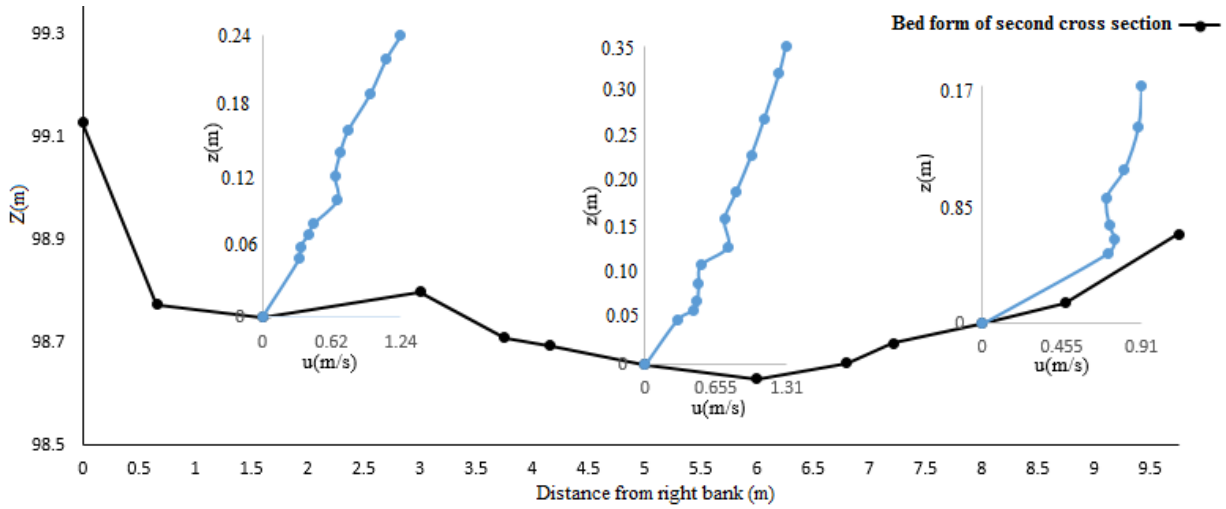

Figure 5. Velocity profiles of the second cross section

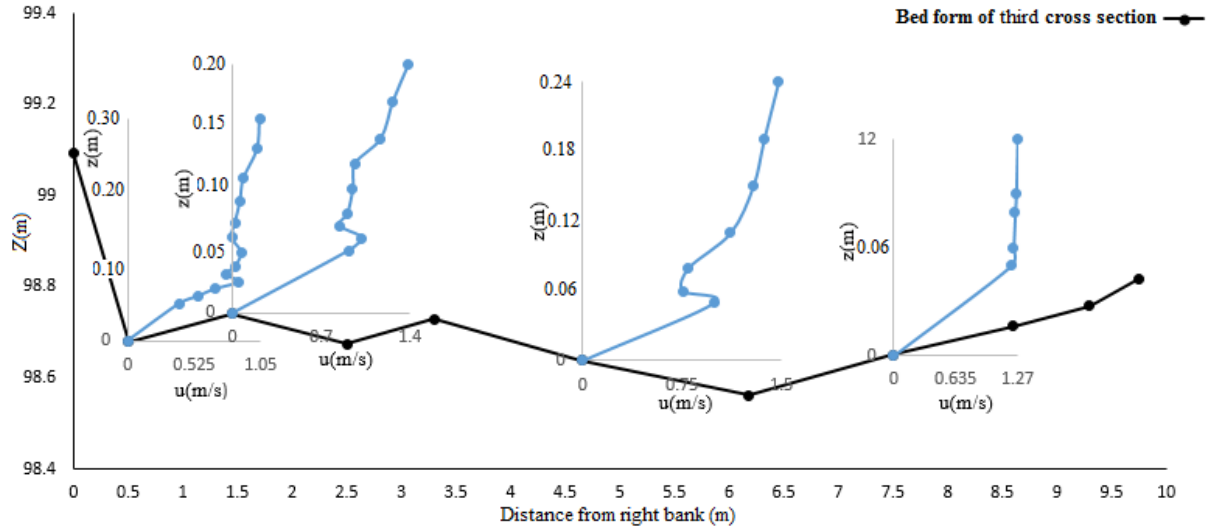

Figure 6. Velocity profiles of the third cross section

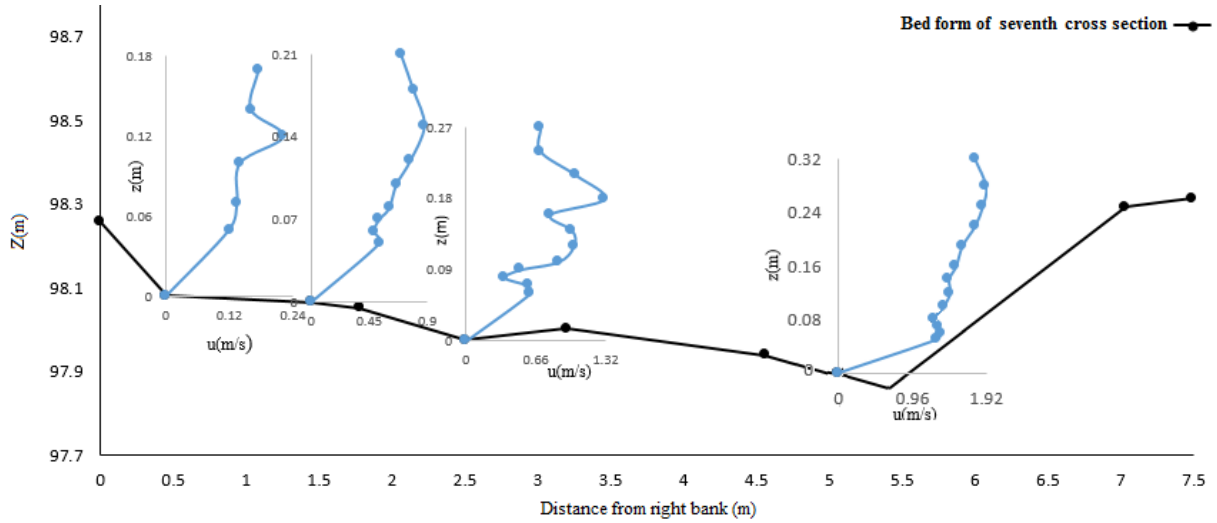

Figure 7. Velocity profiles of the seventh cross section

3. Results and Discussion

3.1. Hydraulic Parameters

Eight cross section were selected in this experimental study to measure the mean velocity points. The measured and calculated parameters in each cross section are mean velocity (U), depth (h), cross section width (W), Reynolds number ($\mathrm{Re} = \frac{\rho U D}{\mu}$) which D is the hydraulic depth which is considered as the flow depth in the channels with large aspect ratio and Froude number ($Fr = \frac{U}{(gD)^{0.5}}$) (Table 1). Reynolds number and Froude number in all cross sections, show that the flow is turbulence and subcritical flow.

As shown in the figure 4, the selected reach has vegetated bank where in some sections vegetation is much dense in the banks. The velocity profile of second, third and seventh cross sections are presented in the figures 5, 6 and 7, respectively.

As shown in the figures 5, 6 and 7, the velocity profiles, especially near the vegetation canopies, have S-shaped distribution. Also, the inflexion point is observed in most of the velocity profiles near the vegetated banks. Since the flow is decelerating and the bed is not flat, the velocity profiles of the middle axis are disorders showing an inflexion point. The inflexion point of velocity profiles occurs at $0.35 < \frac{z}{h} < 0.45$. However, the vegetation in the banks causes the inflexion point moves to higher depth from the bed. Also, the dip phenomenon (the ratio of width to flow depth) occurs near the right bank of the seventh cross section where the dense vegetation is prevalent (figure 7). At the third cross section, the axis with 0.5m distance from the right bank, D3-0.5, was located near the dense vegetated bank where due to strong secondary currents, the mean velocity U=0.5 m/s, is lower than other axis of this section. The secondary flow dominates in lateral direction and the maximum velocity occurs at axis 4.65m away from the right bank, U=1.03 m/s. The flow depth gets low near the left bank of the third cross section and the flow velocity increases suddenly for this region. Also, in this region (axis, D3-7.5), the turbulence is high and the Froude number is Fr=0.9146, which is close to the critical conditions, leading to a specific

velocity distribution which is different from those observed in gravel-bed rivers. One meter upstream of the right bank of the seventh cross section placed a boulder and vegetation density was high around it. After the boulder and the vegetation canopies, the width of the river gets smaller and so that velocity increases at the seventh cross section, except axes which is located 1.5 meter away from the right bank. The lateral velocity gradient is high in the seventh cross section, forcing the strong shear layer emerges around the 1.5-2 m distance from the right bank. Therefore, the velocity profile of axis of 2.5 m distance of the right bank, D7-2.5, shows much disorders and the maximum velocity falls below the water surface, $\frac{z}{h} = 0.66$.

3.2. Shear Velocity

As mentioned in section 2.2., the boundary layer characteristics method and the parabolic method were used to calculate shear velocity in this study. Results show that the parabolic method is acceptable with R^2>0.95, in the outer region of the boundary layer of the measured velocity profiles. However, the correlation coefficient of the velocity profiles used for the parabolic method decreases near the vegetated banks. Figure 8 shows the application of the parabolic method for the measured velocity profiles. As is clear from the figure 8b, the outer layer of the velocity profile of the seventh cross section near the right bank, D7-1.45, did not follows the parabolic method as good as outer regions of the velocity profiles which weren't near the dense vegetation, e.g., D6-3.5.

The shear velocity and shear stress values, $\tau = \rho u^{*2}$, of the selected reach are presented in table 2. Because of the low vertical velocity gradient, the shear velocity and shear stress near the vegetated bank are lower than other axis of each cross section. Also, the bank stability of these region was higher than other regions. Therefore, the width of cross section where the vegetated bank is prevalent shows smaller than other cross sections.

Table 1. The hydraulic parameters and calculated data of selected cross sections

Section name	h (m)	W (m)	Distance from right bank (m)	U (m/s)	Re	Fr	Vegetation presence
D1-1.6	0.20	9.50	1.60	0.9436	188720	0.673656	Sparse
D1-3.2	0.20	9.50	3.20	0.7274	145480	0.519307	-
D1-4.7	0.30	9.50	4.70	0.9363	280890	0.545783	-
D1-6.3	0.32	9.50	6.30	0.9894	316608	0.558422	-
D1-7.9	0.18	9.50	7.90	0.6865	123570	0.516618	Sparse
D2-1.6	0.24	9.75	1.60	0.6476	155424	0.422053	Dense
D2-5	0.35	9.75	5.00	0.7712	269920	0.416197	-
D2-8	0.17	9.75	8.00	0.6743	114478	0.521452	-
D3-0.5	0.30	9.75	0.50	0.4990	149700	0.290874	Dense
D3-1.45	0.20	9.75	1.45	0.9283	185660	0.662733	Sparse
D3-4.65	0.24	9.75	4.65	1.0253	246072	0.668207	-
D3-7.5	0.11	9.75	7.50	0.9501	104511	0.914615	-
D4-0.75	0.32	7.60	0.75	0.7195	230240	0.406089	Dense
D4-2.2	0.22	7.60	2.20	1.0903	239866	0.742164	-
D4-3.8	0.20	7.60	3.80	1.3978	279560	0.99792	-
D4-5.6	0.12	7.60	5.60	0.6994	83928	0.644615	Dense
D5-1.25	0.26	7.30	1.25	0.4127	107302	0.258412	Sparse
D5-3.65	0.26	7.30	3.65	1.4133	367458	0.884939	-
D5-5.9	0.10	7.30	5.90	0.6497	64970	0.655962	-
D6-1.2	0.16	7.00	1.20	0.6705	107280	0.535185	Sparse
D6-3.5	0.26	7.00	3.50	1.0643	276718	0.666412	-
D6-5.8	0.15	7.00	5.80	0.3729	55935	0.307406	-
D7-0.5	0.17	7.80	0.50	0.1151	19567	0.089128	Dense
D7-1.45	0.21	7.80	1.45	0.6118	128478	0.426251	sparse
D7-2.5	0.27	7.80	2.50	0.7415	200205	0.455612	-
D7-5.1	0.32	7.80	5.10	1.4582	466624	0.823015	Sparse
D8-1.8	0.31	7.80	1.80	0.8996	278876	0.515863	Dense
D8-2.2	0.23	7.80	2.20	0.1332	30636	0.088676	-
D8-5.1	0.32	7.80	5.10	1.4689	470048	0.829054	-
D8-6.3	0.30	7.80	6.30	0.8101	243030	0.472219	sparse

Note: D1-1.6 means the ax located 1.6 m far from the right bank of the first cross section.

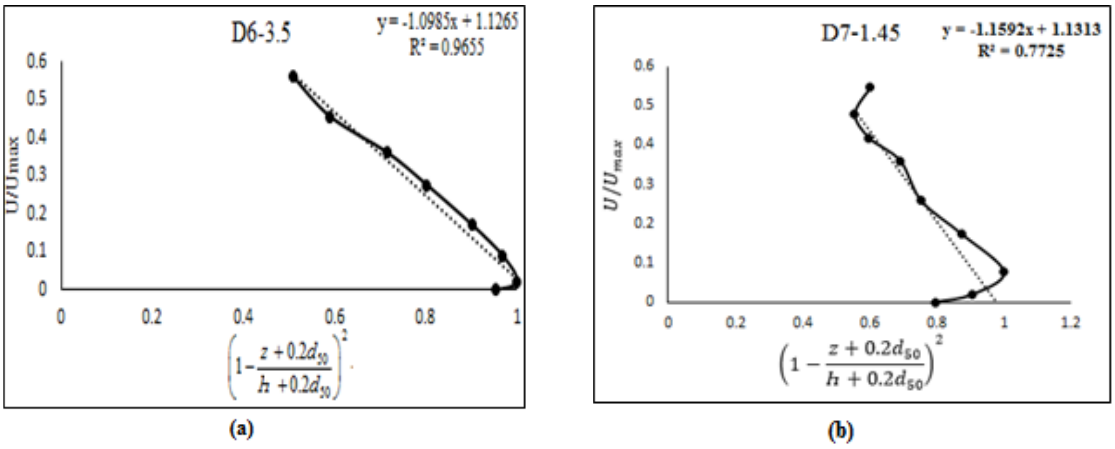

Figure 8. The application of parabolic method with and without vegetated banks

Table 2. Shear velocity and shear stress calculated from boundary layer and parabolic methods

Section name	U (m/s)	Shear velocity (parabolic) (m/s)	Shear velocity (boundary layer) (m/s)	Shear stress (parabolic) (N/m^2)	Shear stress (boundary layer) (N/m^2)
D1-1.6	0.9436	0.1443	0.1523	20.8225	23.1953
D1-3.2	0.7274	0.1164	0.1779	13.5489	31.6484
D1-4.7	0.9363	0.1463	0.1420	21.4037	20.1640
D1-6.3	0.9894	0.1620	0.1866	26.2440	34.8195
D1-7.9	0.6865	0.1750	0.1044	30.6250	10.8993
D2-1.6	0.6476	0.1093	0.1714	11.9465	29.3779
D2-5	0.7712	0.1294	0.1749	16.7443	30.5900
D2-8	0.6743	0.1569	0.0973	24.6176	9.4673
D3-0.5	0.4990	0.1534	0.1271	23.5315	16.1544
D3-1.45	0.9283	0.1699	0.1509	28.8660	22.7708
D3-4.65	1.0253	0.1711	0.1613	29.2752	26.0177
D3-7.5	0.9501	0.7226	0.1449	522.1508	20.9960
D4-0.75	0.7195	0.098	0.1158	9.6040	13.4096
D4-2.2	1.0903	0.1746	0.1821	30.4851	33.1604
D4-3.8	1.3978	0.6464	0.1747	417.8330	30.5201
D4-5.6	0.6994	0.0226	0.0922	0.5107	8.5008
D5-1.25	0.4127	0.0589	0.0509	3.4692	2.5908
D5-3.65	1.4133	0.3374	0.2101	113.8388	44.1000
D5-5.9	0.6497	0.0787	0.1102	6.2015	12.1440
D6-1.2	0.6705	0.1220	0.1288	14.8840	16.5894
D6-3.5	1.0643	0.1697	0.1921	27.7981	36.9024
D6-5.8	0.3729	0.0445	0.0498	1.9802	2.4801
D7-0.5	0.1151	0.002	0.0304	0.0040	0.9241
D7-1.45	0.6118	0.1063	0.1011	11.2997	10.2212
D7-2.5	0.7415	0.0742	0.1644	5.5056	27.0273
D7-5.1	1.4582	0.3312	0.1858	106.6934	34.5216
D8-1.8	0.8996	0.1347	0.1629	18.1441	26.5364
D8-2.2	0.1332	0.007	0.0205	0.0490	0.4205
D8-5.1	1.4689	0.3421	0.1925	117.0324	37.0562
D8-6.3	0.8101	0.1248	0.1159	15.5750	13.4328

3.3. Estimate Flow Resistance

In this study, the drag coefficient was considered as the flow resistance parameter. After calculating the mean velocity and the shear velocity of each cross section and according to the equation 1, the drag coefficient was determined (table 3). Results reveals that the maximum drag coefficient occurs at the second cross section where the density of vegetation on the both banks are high and the mean velocity is minimum. It is known that the drag coefficient increases as the mean velocity decreases. Also, the Reynolds number affects the drag coefficient and there is an inverse relation between them. Based on our field observations the reason the opposite behavior is that the flow infiltrates below the banks and in high flow conditions, the erosion risk gets high in cross sections without the vegetated banks. However, the vegetated banks remain still stable because of the presence of the dense vegetation and increasing in the flow resistance.

Table 3. Mean Drag coefficient of cross sections

Section name	A_{mean} (m^2)	U_{mean} (m/s)	u^*_{mean} (m/s)	$\tau_{0mean\ (N/m^2)}$	C_D
D1	1.8950	0.8001	0.1436	20.6209	0.0644
D2	2.1237	0.6531	0.1429	20.4204	0.0957
D3	1.6390	0.8708	0.1421	20.1924	0.0532
D4	1.2555	0.9234	0.1347	18.0110	0.0425
D5	1.2615	0.8274	0.1222	14.9328	0.0436
D6	1.1405	0.7073	0.1253	15.7001	0.0627
D7	1.5722	0.8588	0.1326	17.5821	0.0476
D8	1.7792	0.7411	0.1033	10.6709	0.0388

4. Conclusions

The flow resistance estimation is investigated for meandering reach with vegetation banks located in northern Iran.

Results show that near the vegetation with different density, the disordered velocity distribution along the meandering reach. The inflexion point of velocity profiles moves toward the water surface, $\frac{z}{h} \simeq 0.65$ in the presence of the vegetated banks. Also, for large aspect ratio in the selected reach $23 < \frac{W}{h} < 30$, the maximum velocity occurs under the water surface in the presence of the vegetation canopies, enhancing the secondary currents generation across of each section. The parabolic method can be applied to calculate shear velocity near the vegetation banks, however, the correlation coefficient reduces due to difficult conditions to a complex interaction of vegetation-gravel bed in the meandering reach. The additional exerted drag of the vegetation canopies increases the flow resistance. Drag coefficient varies from 0.0338 to 0.0644 depending on vegetation density. Therefore, the largest drag coefficient belongs to the second cross section where the dense vegetation is prevalent in this field study. Also, there is an inverse relation between the Reynolds number and drag coefficient.

The results of this study shows that estimation of the flow resistance by using a method which uses the velocity data far from the bed and near the vegetated banks, the parabolic law, can help to obtain better application drag coefficient in hydraulic models.

REFERENCES

[1] Afzalimehr, H., & Anctil, F. (1999). Velocity distribution and shear velocity behavior of decelerating flows over a gravel bed. *Canadian Journal of Civil Engineering*, *26*(4), 468-475.

[2] Afzalimehr, H., & Subhasish, D. E. Y. (2009). Influence of bank vegetation and gravel bed on velocity and Reynolds stress distributions. *International Journal of Sediment Research*, *24*(2), 236-246.

[3] Camporeale, C., Perona, P., Porporato, A., & Ridolfi, L. (2005). On the long-term behavior of meandering rivers. *Water resources research*, *41*(12).

[4] Green, J. C. (2006). Effect of macrophyte spatial variability on channel resistance. *Advances in Water Resources*, *29*(3), 426-438.

[5] James, C. S., Goldbeck, U. K., Patini, A., & Jordanova, A. A. (2008). Influence of foliage on flow resistance of emergent vegetation. *Journal of Hydraulic Research*, *46*(4), 536-542.

[6] Järvelä, J. (2002). Flow resistance of flexible and stiff vegetation: a flume study with natural plants. *Journal of hydrology*, *269*(1-2), 44-54.

[7] Johannesson, H., & Parker, G. (1989). Velocity redistribution in meandering rivers. *Journal of hydraulic engineering*, *115*(8), 1019-1039.

[8] Li, J., Zhang, M., Jiang, E., Pan, L., Wang, A., Wang, Y., & Jian, S. (2021). Influence of Floodplain Flooding on Channel Siltation Adjustment under the Effect of Vegetation on a Meandering Riverine Beach. *Water*, *13*(10), 1402.

[9] Liu, C., Shan, Y., Liu, X., Yang, K., & Liao, H. (2016). The effect of floodplain grass on the flow characteristics of meandering compound channels. *Journal of Hydrology*, *542*, 1-17.

[10] Luhar, M., Rominger, J., & Nepf, H. (2008). Interaction between flow, transport and vegetation spatial structure. *Environmental Fluid Mechanics*, *8*(5), 423-439.

[11] Meire, D. W., Kondziolka, J. M., & Nepf, H. M. (2014). Interaction between neighboring vegetation patches: Impact on flow and deposition. *Water Resources Research*, *50*(5), 3809-3825.

[12] Mohanty, P. K., Mohanty, L. P., & Khatua, K. K. (2022). Discharge estimation in wide meandering compound channels. *ISH Journal of Hydraulic Engineering*, *28* (sup1), 101-115.

[13] Nepf, H., & Ghisalberti, M. (2008). Flow and transport in channels with submerged vegetation. *Acta Geophysica*, *56*(3), 753-777.

[14] Nikora, V., Larned, S., Nikora, N., Debnath, K., Cooper, G.,

& Reid, M. (2008). Hydraulic resistance due to aquatic vegetation in small streams: field study. *Journal of hydraulic engineering*, *134*(9), 1326-1332.

[15] Pollen, N., & Simon, A. (2005). Estimating the mechanical effects of riparian vegetation on stream bank stability using a fiber bundle model. *Water Resources Research*, *41*(7).

[16] Tahershamsi, A., Majdzadeh Tabatabai, M. R., & Torabizadeh, A. (2018). Field study of flow resistance in step-pool streams (case study of Dizin River). *Scientia Iranica*, *25*(5), 2537-2549.

[17] Wolman, M. G. (1954). A method of sampling coarse river-bed material. *EOS, Transactions American Geophysical Union*, *35*(6), 951-956.

[18] Zong, L., & Nepf, H. (2010). Flow and deposition in and around a finite patch of vegetation. *Geomorphology*, *116*(3-4), 363-372.